NACA RM E57C15

NACA

RESEARCH MEMORANDUM

EXPERIMENTAL INVESTIGATION OF MODIFIED CAST-CORED BLADES HAVING HOLLOW TIP SECTIONS

By Robert E. Oldrieve and John C. Freche

Lewis Flight Propulsion Laboratory
Cleveland, Ohio

NATIONAL ADVISORY COMMITTEE
FOR AERONAUTICS

WASHINGTON

June 3, 1957
Declassified December 13, 1957

NATIONAL ADVISORY COMMITTEE FOR AERONAUTICS

RESEARCH MEMORANDUM

EXPERIMENTAL INVESTIGATION OF MODIFIED CAST-CORED BLADES HAVING HOLLOW TIP SECTIONS

By Robert E. Oldrieve and John C. Freche

4466

CA-1

SUMMARY

In order to reduce the weight and root centrifugal stress of cast-cored turbine blades with many small coolant passages near the airfoil surface, fabrication techniques were developed to provide such blades with hollow tip sections. Two types of modified cast-cored blades that provided an 11-percent weight reduction from a fully cast-cored blade (23-percent reduction in root centrifugal stress) and a 13-percent weight reduction from a standard uncooled blade were investigated in a turbojet engine modified for air-cooling. One blade configuration had 37 (0.060-in.) coolant passages, and the other had 20 oval passages (0.100 by 0.060 in.), extending from the root to 9/16 span. Both blades were hollow from 9/16 span to the tip; the 37-hole blade was a one-piece casting, and the 20-hole blade had a brazed-on hollow tip section of formed sheet metal.

At rated engine speed (11,500 rpm) and a turbine-inlet gas temperature of 1740° F, the 37-hole blade showed surface temperatures 30° to 70° lower and metal core temperatures 100° to 165° F lower than the 20-hole blade over a coolant-flow-ratio range from 0.015 to 0.072 at the midspan position. Endurance operation at the same speed and gas temperature at a coolant-flow ratio of 0.005 resulted in failure of the 20-hole blade in the tip section after $4\frac{1}{2}$ hours. One 37-hole blade showed cracks in the tip section along one of the stiffeners after $9\frac{1}{4}$ hours, and a second blade was operated without failure for 25 hours. Local blade temperatures (surface and metal core) calculated for the 37-hole blade with an electric analog agreed reasonably well with experimental values over most of the coolant-flow range.

Cooling-air total-pressure drop obtained in a stationary test was 62 percent lower for the 37-hole blade and 33 percent lower for the 20-hole blade than that of a corrugated-insert blade with 0.050- by 0.050- by 0.005-inch corrugations at a coolant flow of 0.02 pound per second. Calculated and experimental pressure-drop values agreed reasonably well at low coolant-flow rates likely to be encountered in cooled-engine operation.

INTRODUCTION

The weight of fully cast-cored blades (one-piece cast blades with many small coolant passages near the airfoil surface extending through the entire blade) can be reduced by making the upper portion of the blade hollow. This investigation was conducted at the NACA Lewis laboratory primarily to determine the heat-transfer and pressure-loss characteristics of two blade configurations of this type.

A great deal of the NACA turbine-cooling research has dealt with cooled blades that employed brazing to unite the blade shell and base. In order to provide an alternate fabrication method as well as one that eliminates brazing in the highly stressed root region, a one-piece cast blade with many small coolant passages near the airfoil surface was developed (ref. 1). Similar cooling configurations have been investigated by the British, who used casting, sintering, and forging procedures (refs. 2, 3, and 4, respectively). An undesirable feature of this type of blade configuration, however, is its relatively high weight (ref. 1). A method of reducing this weight disadvantage is to make the blade tip section hollow, as suggested in reference 1, and to modify the cast-cored blades as reported herein.

This report presents (1) experimental cooling results, (2) comparison of experimental and calculated blade temperatures, (3) blade cooling-air pressure-drop data, and (4) a limited amount of endurance data. The coolant passages in the lower portion of one of the blade configurations investigated consisted of 37 (0.060-in.) holes. The other configuration had 20 oval passages with a 0.100-inch major axis and a 0.060-inch minor axis. The blades were investigated in a turbojet engine altered to accommodate two air-cooled blades. Heat-transfer data were obtained over a range of cooling-air flows at a constant engine speed of 11,500 rpm (rated speed), an average turbine-inlet gas temperature of 1740° F, and coolant- to gas-flow ratios of approximately 0.008 to 0.073. Endurance operation was conducted briefly with both the 37-hole and the 20-hole blades at rated engine speed (blade root centrifugal stress approx. 31,200 psi), a turbine-inlet gas temperature of 1740° F, and a coolant-flow ratio of 0.005.

SYMBOLS

A	cross-sectional flow area, sq ft
b	blade span, ft
c_p	specific heat at constant pressure, Btu/(lb)(°F)
d	diameter, ft

4466

E	electromotive force, volts
g	acceleration due to gravity, 32.2 ft/sec^2
h	heat-transfer coefficient, Btu/(sec)(sq ft)($^\circ$F)
K_C	contraction coefficient
K_E	expansion coefficient
k	thermal conductivity, Btu/($^\circ$F)(ft)(sec)
l	length, ft
M	Mach number
P	total pressure, lb/sq ft
p	static pressure, lb/sq in. or lb/sq ft
S	surface area, sq ft
T	total temperature, $^\circ$F or $^\circ$R
t	temperature, $^\circ$F or $^\circ$R
V	velocity, ft/sec
w	weight flow, lb/sec
x	distance along blade span or from cooling-passage entrance, ft
γ	ratio of specific heats
ρ	density of air, lb/cu ft
φ	cooling-effectiveness parameter, $(\overline{t}_{g,e} - \overline{t}_{b,l})/(\overline{t}_{g,e} - \overline{T}_{a,in})$

Subscripts:

a	blade cooling air
b	blade
bar	barometric conditions
e	effective

4466 CA-1.back

g	combustion gas
i	inside (coolant side)
in	inlet
l	local point or span location
o	outside (gas side)
std	standard atmospheric conditions
1,2,3 4,5,6	blade stations (fig. 7)

Superscript:

	average value

4466

BLADE DESCRIPTION AND FABRICATION

The cooled blades had a span of 4 inches, a chord of 2 inches, and were twisted from root to tip. One blade type, a one-piece casting of HS-31 alloy, was provided with 37 (0.060-in.) holes in the lower blade portion along the blade profile. The upper blade section was a hollow shell tapered from 0.036 to 0.021 inch. A second blade type had 20 oval holes (0.100 by 0.060 in.) in the lower blade portion. The cast portion of this blade was HS-31 and the hollow tip region L-605 formed sheet; these portions were brazed together at the 9/16-span position. The hollow-shell section was untapered and had a thickness of 0.020 inch. In each case the final blade profile was identical to that of the cast-cored blade (ref. 1), the same casting dies having been used. Each of the blades weighed approximately 0.73 pound, an 11-percent reduction in weight from the fully cast-cored blade of reference 1 and a 13-percent reduction from a standard uncooled blade.

The blades were made by precision-investment casting, using the lost-wax process. Basically, the procedure was the same as that described in reference 1 for the fully cast-cored blade. Because the blades were hollow from the 9/16-span position to the tip, certain additional techniques were required. It should be emphasized that the casting procedure described is not suitable for mass production and was used only because relatively few blades were required. By use of the following procedure, considerable savings were realized, in that new dies for making waxes were not required.

4466

A wax duplicate of a hollow blade (fig. 1(a)) was made using available dies (ref. 1) for this blade profile. The upper portion (from the 1/2-span position to the tip) was cut off and split along the leading and trailing edges into two sections as shown in figure 1(b). Each section was placed in its appropriate die half (fig. 2(a)) and coated with oil to prevent additional wax from adhering to its surface. Two strips of pattern wax, approximately 3/8 inch wide by 0.030 inch thick, were also placed in each die half as shown in figure 2(b); and commercially available hollow mullite (ceramic) cores were laid adjacent to each other and lightly pressed into the wax strips (also shown in fig. 2(b)). Thirty-seven 0.060-inch round cores approximately 0.011 inch apart were used for one type of blade, and 20 hollow oval cores with a major axis of 0.100 inch and a minor axis of 0.060 inch approximately 0.035 inch apart were used in the second type of blade.

The two die halves were next joined and filled with molten wax under pressure. Upon hardening, the completed wax pattern was removed from the die (fig. 3(a)). The shoulder in the wax pattern at approximately 1/2 span is present because the wax that was injected into the mold did not adhere to the oil-coated wax shells previously placed in the dies. The wax in the upper portion of the blade was melted off with a hot iron to within 1/2 inch of the shoulder, as shown in figure 3(b). The final wax pattern (fig. 3(c)) was achieved by slipping a hollow wax shell corresponding to the upper portion of the blade profile over the exposed mullite cores until it butted with the shoulder on the lower portion of the wax pattern. A filler wax was used to make the junction smooth. The rest of the casting and core-removal procedure was identical to that described in reference 1.

Another major variation of the fabrication process described was also employed. This consisted in casting only the lower portion of the blade and providing the hollow tip region by brazing a formed hollow shell to the cast portion of the blade. To achieve this result, the steps in making the wax pattern ended with that shown in figure 3(b). This pattern was then invested, and the normal casting and core-removal procedure followed. A formed hollow shell was then fitted and brazed to the casting.

Both types of blade were provided with two ribs in the hollow tip section. These are shown in a tip-view photograph of a completed blade (fig. 4). These ribs extended into the hollow section about 1 inch and served as stiffeners to prevent "oil-canning" of the hollow tip. The stiffening members were made of sheet metal about 0.025 inch thick and brazed in position.

APPARATUS AND INSTRUMENTATION

Engine Modifications

Engine modifications are described in detail in reference 5, except for the balanced-pressure sliding seal that was used to transfer pressurized cooling air from an external source (laboratory service air system) to the turbine rotor. The seal mechanism (described in ref. 6) was substituted for the labyrinth seal used in previous installations because it eliminated cooling-air leakage between stationary and rotating components of the cooling-air system. Consequently, no cooling-air leakage calibration was required as in previous investigations.

4466

Blade and Engine Instrumentation

The test blades were instrumented with thermocouples as shown in figure 5. The surface thermocouples were buried in the blade to a depth of approximately 0.010 inch by the method described in reference 7. A piece of 0.005-inch-thick sheet metal was tack-welded over the ceramic surrounding the thermocouple wires in order to eliminate erosion. The blade surface was sufficiently recessed so that the sheet metal did not extend above it and mar the aerodynamic contour. Figure 5(a) illustrates the manner in which the 37-hole blade was instrumented. In order to obtain a complete temperature survey, the blade was instrumented in each of the three ways shown in the figure. The 20-hole blade was instrumented in each of the two ways shown in figure 5(b).

In order to obtain the effective gas temperature (uncooled-blade temperature), several standard uncooled blades were provided with thermocouples along their leading edges at various spanwise positions, as shown in figure 5(c). Two of these blades were cut off at approximately the 2/3-span position to reduce centrifugal stress, thereby reducing the possibility of early failure due to the metal removal required for thermocouple installation. The reference blade with the thermocouple at $1\frac{1}{2}$-inch span was used during all the test runs. The reference blade with thermocouples at the 2- and $2\frac{1}{2}$-inch-span positions was used during the runs in which cooled-blade heat-transfer data were being obtained at these same span positions. The reference blade with the root and tip thermocouples was used when cooled-blade root and tip or central metal core heat-transfer data were obtained.

Engine speed, airflow, fuel flow, cooling airflow and temperature, and tailpipe gas temperature were all measured as described in reference 5.

4466

EXPERIMENTAL PROCEDURE

Heat-Transfer Investigation

Each of the two types of test blades was operated separately. The 37-hole blade, instrumented in one of the ways shown in figure 5(a), was installed in the test engine, and blade temperature data were determined at an engine speed of 11,500 rpm (rated) and a turbine-inlet gas temperature of 1740° F (effective gas temperature of approx. 1500° F). Coolant-flow ratio was varied over as wide a range as the experimental installation permitted, from 0.008 to 0.073. Blade cooling-air pressure drop and the service-air supply pressure limited the maximum coolant flow. Upon completion of such a series of runs, the test blade was reinstrumented in another of the ways shown in figure 5(a) and retested at the same set of operating conditions. The 20-hole blade was operated in the same manner, and the range of coolant-flow ratios covered was from 0.015 to 0.073.

Blade Pressure-Drop Determination

The total-pressure drop through the test blades was obtained in a stationary test using the mockup section of the turbine rotor instrumented as described and illustrated in figure 10(a) of reference 8. The over-all total-pressure drop through the blade base and the blade aerodynamic section was obtained for an approximate range of air weight flows from 0.003 to 0.050 pound per second in several increments.

Structural-Reliability Investigation

A limited amount of endurance operation was conducted with both blade types at rated engine speed, a coolant-flow ratio of 0.005, and a turbine-inlet gas temperature of 1740° F. The calculated average centrifugal stress (blade root) at this speed was approximately 32,100 psi for each blade. The gas temperature was identical to that set during the heat-transfer runs, and the coolant-flow ratio was slightly lower than the lowest set during the heat-transfer runs. A coolant-flow ratio of 0.005 closely approximates that set during one phase of the endurance investigation with a fully cored blade (ref. 1). Also, such a flow ratio is in keeping with desired low-coolant-flow requirements in cooled-turbojet-engine applications.

CALCULATIONS

Heat Transfer

Surface and metal core temperatures. - The midchord surface and metal core temperatures at both the root and the 2-inch-span position of

the 37-passage blade were determined with the use of an electric analog. These calculated temperatures are compared with experimental values in the RESULTS AND DISCUSSION section.

A cross section of the 37-passage cast-cored blade is illustrated in figure 6(a). A simple one-dimensional analog was designed for a typical blade section, such as that between lines A-A, B-B, and C-C of the figure. The resistance-network diagram for this section, shown in figure 6(b), is similar to that presented in figure 9 of reference 9 for a strut-blade analysis. Use of such a partial blade analog is made possible by the assumed symmetry of the heat-flow paths, as shown in figure 6(c). The network diagram (fig. 6(b)) should be applicable for determining local temperatures throughout the greater portion of the blade enclosed by lines D-D and E-E of figure 6(a) by the introduction of appropriate resistances. At the blade leading and trailing edges a grid-type network such as shown in figure 21 of reference 9 is more applicable because of the lack of heat-flow symmetry in these areas.

4466

Construction details and the method of analog application are described in reference 9. Briefly, electrical resistances were determined so that, at any local point in the heat-flow path, the heat-flow-path resistance to a point divided by the over-all heat-flow-path resistance equaled the electrical resistance to the corresponding point divided by the over-all electrical resistance of a simulated electrical flow path. Thus,

$$\frac{\Delta t_l}{\Delta t} = \frac{t_{g,e} - t_l}{t_{g,e} - T_{a,l}} = \frac{\Delta E_l}{\Delta E} \tag{1}$$

If an over-all change in potential ΔE is imposed on the electrical network and ΔE_l is measured at any station, the temperature t_l at that station can be determined from equation (1) when the over-all temperature difference of the system Δt (difference between gas and coolant temp.) is known. Terms representing thermal resistance for each element in the heat-flow path are shown in figure 6(b).

Heat-transfer coefficients. - The gas-to-blade heat-transfer coefficients employed in the analog calculations were an average of the local midchord values on the pressure and suction surfaces theoretically determined by the method of reference 10. Blade velocity profiles required in this determination were obtained from stream-filament theory as described in reference 11.

Local blade-to-coolant heat-transfer coefficients were finally evaluated by the following equation of reference 12, which accounts for entrance effects in the blade coolant passages:

$$\frac{h_l d}{k} = 1.16\left(31 + \frac{wc_p}{kx}\right)^{1/3} \qquad (2)$$

Some of the coolant-flow Reynolds numbers exceeded 2300, indicating flow in the transition region between laminar and turbulent flow. One Reynolds number exceeded 10,000. These flow conditions would normally indicate the use of coefficients obtained from the correlation of figure 2 of reference 13 or figure 8 of reference 14. This was attempted, and the results are discussed in the RESULTS AND DISCUSSION section. Film temperatures were used to obtain the fluid properties needed to evaluate the blade-to-coolant coefficients. Coolant temperatures at local spanwise locations were obtained by the iterative solution outlined in reference 9.

4466

Stress

Centrifugal stress at any spanwise section was based upon total metal area at the station considered. For each blade type, root centrifugal stress was about 32,100 psi, approximately 23 percent lower than that of the fully cored blade of reference 1. The allowable stress for the cored portion was determined from the average experimental blade temperature (weighted on an area basis as in ref. 1) at the spanwise station considered and stress-rupture or yield-strength data, whichever was applicable, for the blade material. For the hollow tip region, the allowable stress was similarly determined using an integrated average experimental blade shell temperature at the station considered.

CA-2

Pressure Drop

The over-all total-pressure drop through both of the blade types investigated was calculated for comparison with experimental data. The calculation procedure was for the following conditions: no rotation, no coolant temperature rise through the blade, and a static pressure at the blade tip (stations 1 and 2, fig. 7) equal to barometric pressure. Figure 7 illustrates the various stations discussed in the calculation procedure. The stations are numbered to indicate the sections of the blade that required a specific calculation method (the calculation progressed from the known conditions at the blade tip to the measured pressure at station 6). The sections were subdivided, when necessary, to provide greater accuracy in the calculation procedure.

The total pressure at the blade tip (station 2) was determined from the known area, weight flow, static pressure, and total temperature. The total and static pressures and Mach number at station 3 were found by use of the charts of reference 15. Next, the total-pressure loss across the

junction between the hollow portion and the cored portion of the blade (stations 3 to 4) was determined by the Carnot-Borda relation, which may be expressed as

$$\Delta P = K \frac{\rho V^2}{2g} \tag{3}$$

For a sudden expansion the coefficient K_E may be expressed in terms of the flow areas so that equation (3) becomes

$$\Delta P_{3-4} = K_E \frac{\gamma p_3 M_3^2}{2} = \left(\frac{A_3}{A_4} - 1\right)^2 \frac{\gamma p_3 M_3^2}{2} \tag{4}$$

Although this relation assumes fluid incompressibility and no density change between successive stations, it is expressed in terms of Mach number, which is the working parameter of the charts of reference 15. The change in total pressure through the cored portion of the blade (stations 4 to 5) was then determined, again using the charts of reference 15. From these charts it is also possible to obtain the static pressure and Mach number at station 5.

The loss due to the sudden contraction that occurs in the blade base region (between stations 6 and 5) was obtained from an equation similar to equation (4), in which the expansion coefficient K_E was replaced by a contraction coefficient K_C. A sudden contraction produces losses that can be determined completely only with the help of experimentally determined coefficients. The contraction coefficient K_C was obtained from figure 52 of reference 16. The total-pressure drop through the blade was corrected to standard conditions by multiplying by a density ratio ρ_{bar}/ρ_{std}.

RESULTS AND DISCUSSION

Experimental Heat-Transfer Results

Chordwise blade surface temperature distributions in the 37-passage blade for rated-speed operation are shown in figure 8 for three of the span locations investigated. Since incomplete temperature data for the fourth span location at the extreme tip of the blade (see fig. 5(a)) resulted from thermocouple failures, a chordwise temperature plot was not made. The coolant-flow ratios and corresponding blade cooling-air inlet temperatures are indicated in the figure. The effective gas temperature (uncooled-blade temperature) at each spanwise station is included. At the lowest nominal coolant-flow ratio common to both the 37- and 20-passage blade heat-transfer tests (0.015), the midchord suction-surface blade temperatures of the 37-hole blade were lower than the

4466

local effective gas temperature by 325° F at the root (fig. 8(c)), 236° F at the 2-inch span (fig. 8(b)), and 185° F at the $2\frac{1}{2}$-inch span (fig. 8(a)). The reductions in pressure-surface temperatures were of similar magnitudes. The maximum chordwise temperature differences for the 0.015 coolant-flow ratio were 260° F at the root and 170° F at the 2-inch span.

Figure 9 shows chordwise blade temperature distributions for the 20-passage blade. At the coolant-flow ratio of 0.015, the midchord suction-surface blade temperatures were lower than the local effective gas temperature by 88° F at the 2-inch span (fig. 9(b)) and 108° F in the hollow shell at the $2\frac{1}{2}$-inch span (fig. 9(a)).

The change in average surface temperature and midsection metal core temperature with coolant-flow ratio at rated engine speed is shown for the 2-inch-span and root stations of the 37-passage blade and for the 2-inch span of the 20-passage blade in figure 10. At the coolant-flow ratio of 0.015 the surface to core temperature difference for the 37-passage blade was 250° F at the root and 235° F at the 2-inch span. For the 20-passage blade this difference was 145° F at the 2-inch span. The general temperature level of the 37-hole blade is lower (100° to 165° in the central core region and 30° to 70° on the surface) at the 2-inch span than that of the 20-hole blade over the coolant-flow-ratio range covered. A low metal temperature in the central portion of the blade is of course desirable, since it represents a large part of the blade stress-supporting area. It should be noted, however, that low central-region temperatures accompanied by high surface temperatures make uncertain the determination of the metal temperature upon which allowable stress calculations should be based. Furthermore, such temperature differences introduce thermal stresses that further complicate the design problem. As a result of these factors, it should not be concluded that the 37-hole blade would be more desirable than the 20-hole blade in all applications. Thermal stresses were not evaluated in this investigation.

Average blade metal temperatures for all spanwise thermocouple locations are plotted in figure 11 for the 37-passage blade. Also shown is a detailed spanwise distribution of effective gas temperature. This was obtained largely from measured reference blade temperatures of these tests and partly from unpublished NACA data from engines of the same model. The average temperatures were obtained from integrated average surface temperatures and midsection metal temperatures weighted on a blade metal area basis. The incomplete chordwise temperature data obtained at the tip were similarly averaged in this instance to provide the tip-section data shown in the figure. The blade metal temperature rise across the junction between the cored and hollow sections of the blade was 70° F in a distance of 1/2 inch at a coolant-flow ratio of 0.015 and increased to 150° F at the maximum flow ratio (0.072). No

4466
CA-2 back

significant difference in temperature between the 0.625 span position and the tip occurred except at the maximum flow ratio, indicating low cooling effectiveness for the hollow blade portion, as expected.

No thermocouples were available at the root or tip of the 20-passage blade; therefore, a similar plot for this blade could not be made. However, figures 9 and 10 show that the temperature increase from the 2- to $2\frac{1}{2}$-inch blade span was generally of the same magnitude as that of the 37-hole modified cast-cored blade. The allowable blade temperature curves superimposed on figure 11 are discussed in connection with the endurance operating results.

4466

Temperature Comparison with Other Cooled-Blade Configurations

The cooling characteristics of the 37-passage modified cast-cored blade are compared in figure 12 with a strut blade, a corrugated-insert blade, and a simple hollow blade on the basis of the nondimensional blade cooling-effectiveness parameter φ. The parameter φ is defined as the difference between the local effective gas temperature and the average blade metal temperature at a particular spanwise station divided by the difference between the effective gas temperature at the station and the blade inlet cooling-air temperature. The blades are compared at the 1/3-span location for rated engine speed and turbine-inlet gas temperatures ranging from 1655° to 1740° F over a range of coolant-flow ratios from 0.008 to 0.080. The 5/8-span location of the 37-passage blade is also shown for the same operating conditions. The corrugated-insert and hollow-blade data were obtained from unpublished NACA results, and the strut-blade data from reference 17.

The corrugation amplitude, pitch, and thickness were 0.070, 0.070, and 0.007 inch, respectively, for the corrugated-insert blade. Since strut temperatures (the stress-supporting member) were employed for the strut blade, its cooling effectiveness is the greatest. The corrugated-insert blade with its large amount of heat-transfer surface area shows the next highest effectiveness, followed by the 37-hole modified cored blade (1/3 span), the hollow blade, and the hollow section of the 37-hole blade. It is reasonable to expect the effectiveness parameters to be slightly lower for the hollow section of the 37-hole blade than those determined for the simple hollow blade, because the spanwise position considered is greater and the blade temperatures would naturally be higher.

It should be noted that only the modified cored blades were operated with a nonleakage cooling-air seal. Consequently, the other blade data (taken before the nonleakage seal was available) are subject to the accuracy of the cooling-air leakage calibration, which is frequently a large

percentage of the total flow, particularly at low coolant-flow rates. In the low-coolant-flow range, the curves for these blades may shift; however, the results shown are qualitatively correct. With these effective curves it is possible to determine blade temperatures at any coolant-flow ratio for similar engine mass flows and blade sizes. It is not advisable, however, to extrapolate to gas-temperature levels many hundreds of degrees in excess of that at which these data were obtained.

4466

Calculated and Experimental Blade Temperatures

Calculated and experimental blade temperatures are compared for the 37-hole blade in figure 13 at rated engine speed and a turbine-inlet gas temperature of 1740° F. The range of coolant-flow ratios covered is from 0.008 to 0.072. Only this blade is compared because more complete instrumentation and data are available. Experimental blade metal core temperatures at both the root and the 2-inch-span stations are compared with calculated values in figure 13(a). The averages of the experimental midchord surface temperatures on the pressure and suction surfaces are compared with calculated midchord surface temperatures in figure 13(b). Reasonable agreement was obtained over most of the flow range. The maximum deviation of a calculated metal core temperature from the experimental value was 130° at a measured temperature of 800° F, at the 2-inch-span position. Calculated midchord surface temperatures show considerably better agreement with experimental values. The maximum deviation between calculated and experimental values in this case was about 130° at a measured temperature of 990° F. The point of maximum error represented the highest-coolant-flow run and a coolant-flow ratio of approximately 0.072, which is probably unrealistic with respect to cooled-engine operation.

The degree of agreement between calculated and experimental results may be affected by several factors, one of which is the value of the cooling-air temperature. The fact that this was calculated for the 2-inch-span position, not experimentally measured as at the root, may contribute to the more unfavorable comparison obtained at the 2-inch span. Another factor affecting the final calculation accuracy is the blade-to-coolant heat-transfer coefficient. As previously stated, the coolant-flow Reynolds number in several instances exceeded 2300 and in one case exceeded 10,000. Use of coefficients generally considered applicable to the transition and turbulent-flow regions caused the calculated temperature values to fall considerably below the 45° correlation line. Owing to boundary-layer growth near the passage entrance, a high average Reynolds number (based on passage diam.) does not guarantee the existence of turbulent-flow coefficients in the passage entrance region. Because of the foregoing considerations, use of laminar-flow coefficients particularly at the root of the blade (entrance effects most pronounced) appears applicable for this investigation in light of the agreement achieved with experimental data.

Cooling-Air Pressure Drop

Calculated and experimental values. - Values of calculated and experimental blade cooling-air total-pressure drop are compared in figure 14 for the modified cored blades investigated herein and for the fully cast-cored blade of reference 1. The latter blade had cored passages extending through the entire blade span. In general, the amount of deviation from a 45° line increases with increasing blade pressure drop. The maximum difference between calculated and experimental values, approximately 30 percent, occurs at the highest value of pressure drop (max. coolant-flow rate). However, at the lower coolant-flow rates, which are more likely to be encountered in cooled-engine operation, reasonable agreement was achieved.

4466

The 30-percent error in calculated pressure drop at the high weight flows indicates that compressibility effects may reach appreciable magnitudes. In general, it appears that, in calculating cored-blade pressure drop, available contraction loss coefficients for individual tubes may satisfactorily be applied to blades having many small passages with an equivalent flow area. An error in contraction coefficient would affect pressure losses over the entire range of coolant flows. The coefficient as applied herein depended solely upon the area ratio at the contraction. Although the effects of rotation and coolant temperature rise are not included in these calculations, the method is useful to the cooled-blade designer in comparing various blade configurations.

Pressure-drop comparisons. - Figure 15 presents the cooling-air pressure drop through the 20- and 37-passage blades of the present investigation, the fully cored blade of reference 1, a conventional corrugated-insert blade with 0.050-inch corrugations and a second corrugated-insert blade with 0.070-inch corrugations over a range of approximately 0.003 to 0.050 pound per second. The values shown are the over-all total-pressure drop including pressure loss through the base of each blade investigated. The pressure drop through individual passages was not measured.

The magnitude of pressure drop that is acceptable depends, of course, upon the engine application under consideration. For example, at rated-speed operation in the test facility employed, the required coolant weight flow per blade is approximately 0.02 pound per second for a coolant-flow ratio of 0.015. At this flow rate the pressure drop was 6 pounds per square inch through the 0.050- by 0.050- by 0.005-inch corrugated blade, approximately 4 pounds per square inch for both the fully cored and the 20-passage modified cast-cored blades (33 percent lower), and about 2.3 pounds for both the 37-passage modified cast-cored and the 0.070- by 0.070- by 0.007-inch corrugated blades (62 percent lower).

In general, the relative blade pressure-drop level for each configuration fell as expected with the possible exception of the 20-passage half-cored blade and the 0.070- by 0.070- by 0.007-inch corrugated blade. With the large passages of the cored blade and the high theoretical coolant-flow area of the 0.070- by 0.070- by 0.007-inch corrugated blade, somewhat lower pressure drops might be expected. The coolant passages in both blades were known to be partially blocked. For the 20-hole blade, interference of the base serrations with several of the passages caused partial blockage of these passages upon insertion of this blade into the stationary pressure-drop test facility. Partial corrugation blockage by braze material handicapped the corrugated-insert blade. These factors are of course not inherent in the particular designs in question. Quantitatively, the pressure loss through any of these blades is not excessive; however, the conditions of the specific installation must be the determining factor. For example, the cooling-air supply pressure (compressor bleed) should be sufficient to overcome the pressure drop of the cooling-air ducting and the blade and still be greater than the gas pressure at the rotor blade tip. Since the blade pressure drop was determined in a stationary installation at room temperature, the effects of rotation and coolant temperature rise are not included in these results. The values presented nevertheless indicate the blade pressure losses on a qualitative basis with the possible exception of the 20-hole modified cast-cored blade and the corrugated-insert blade (0.070-in. corrugations) for the reasons already discussed.

4466

Structural Reliability

Endurance is evaluated herein from limited structural-reliability data as well as from the results of runs made primarily to obtain heat-transfer data. Endurance operation was conducted for both modified-cored blade types at rated engine speed, a coolant-flow ratio of 0.005, and a turbine-inlet gas temperature of 1740° F. In order to avoid possible weakening of the structure, these blades were not instrumented. The blades operated during the heat-transfer runs were of course instrumented. No blade failures were encountered in regions critical with respect to centrifugal stress during any phase of the current investigation.

As part of the endurance runs one 37-hole blade was operated about 7 hours when a crack first appeared in the hollow shell along one of the brazed-in stiffeners. After the crack was patched with additional braze, engine operation was continued. At a total of $9\frac{1}{4}$ hours of operation, the crack reappeared and operation was discontinued. A second 37-hole blade was operated for 25 hours with no visible damage in any portion of the blade. A 20-hole blade was operated for $4\frac{1}{2}$ hours, when failure occurred in the upper portion of the hollow shell region. During the heat-transfer

runs both blade types failed in the hollow shell region along instrumentation slots. Such a failure (37-hole blade) is shown in figure 16. This failure occurred upon completion of $4\frac{1}{2}$ hours of rated-speed operation and a total operating time of $10\frac{3}{4}$ hours. The 20-hole blade failed in a similar fashion after $2\frac{1}{2}$ hours at rated speed and a total operating time of 5 hours.

As stated previously, engine operation indicated that none of the blades failed at a section made critical because of centrifugal stress. The sections that are critical on this basis are shown graphically for the 37-hole blade in figure 11. In this figure the curves of allowable blade temperature for 100-hour life assuming allowable- to centrifugal-stress ratios of 1.5 and 2 are superimposed upon a plot of average blade temperature against blade span. The critical point, at which the average blade temperature and the allowable temperature curves are closest, is at the root, although the 0.56 span is potentially critical. The proximity of the curve for effective gas temperature to the blade temperature curve at the blade tip, also shown in figure 11, indicates that blades with hollow tip sections may be critical in this region on the basis of temperature only. Although the allowable curves apparently show a wide margin of safety at the blade tip (because of the low centrifugal stress at this point), the inability of the blade to operate at a temperature appreciably lower than the gas temperature at the tip may be a potential source of difficulty. This is particularly true at higher gas-temperature levels. From unpublished NACA data obtained with simple hollow blades it appears that vibratory stress may have been an important factor in the blade failures encountered with the modified cast-cored blades. Certainly, the inability to provide appreciable cooling in the hollow tip region would tend to aggravate the problem already posed by vibration in this region.

On the basis of the results reported herein, it appears that care must be exercised in the removal of blade tip material to acquire reduced root stress and reduction in over-all blade weight. Such a modification cannot be made on the basis of centrifugal-stress considerations alone. The modified cast-cored blades appear to be limited by the strength characteristics of the hollow shell resulting from the combined effects of reduced cooling effectiveness and vibratory stress. By refinement of fabrication techniques, providing greater hollow-shell taper ratio if necessary, and judicious addition of stiffening members, an improved structure may be developed without an appreciable increase in blade weight.

SUMMARY OF RESULTS

The following results were obtained from an experimental investigation of modified cast-cored blades with hollow tip regions:

4466

1. Techniques for making cast-cored blades were extended to provide such blades with hollow tip sections in order to achieve a reduction in cast-cored blade weight and root centrifugal stress. An 11-percent weight reduction from the fully cast-cored blade and a 13-percent reduction from a standard uncooled blade were obtained. Root centrifugal stress was reduced approximately 23 percent from that of the fully cast-cored blade.

2. Of the two modified cast-cored blade configurations investigated, the 37-hole blade cooled more effectively than the 20-hole blade at all spanwise stations investigated. For example, at the 2-inch-span position the temperature difference was 100° to 165° F in the metal core region and 30° to 70° F on the surface during operation over the coolant-flow-ratio range covered at rated speed and a turbine-inlet gas temperature of 1740° F.

3. During structural-reliability runs one 37-hole modified cast-cored blade was operated for $9\frac{1}{4}$ hours and another for 25 hours at rated engine speed (root centrifugal stress, 31,200 psi), a coolant-flow ratio of 0.005, and a turbine-inlet gas temperature of 1740° F without failure. A 20-hole modified cast-cored blade (similar root stress) was operated at the same conditions for $4\frac{1}{2}$ hours, when failure occurred in the hollow shell region. The endurance results indicate that further development of techniques for stiffening the hollow shell portion is required.

4. Local blade temperatures (surface and metal core) were calculated with an electric analog. The maximum difference between calculated and experimental metal core temperatures was 130° F, at a measured temperature of 800° F at the 2-inch-span position. The maximum deviation between calculated and experimental surface temperatures was also about 130° F, at a blade temperature of 990° F.

5. Over-all cooling-air total-pressure drop was less for both of the modified cored blades than for a corrugated-insert blade with 0.050- by 0.050- by 0.005-inch corrugations. A corrugated-insert blade with 0.070- by 0.070- by 0.007-inch corrugations showed about the same pressure drop as the more favorable 37-hole modified cast-cored blade. Reasonable agreement between calculated and experimental blade cooling-air total-pressure drop was achieved by use of available contraction loss coefficients and standard calculation procedures at low coolant-flow rates likely to be encountered in cooled-engine operation.

Lewis Flight Propulsion Laboratory
National Advisory Committee for Aeronautics
Cleveland, Ohio, March 19, 1957

4466 CA-3

REFERENCES

1. Freche, John C., and Oldrieve, Robert E.: Fabrication Techniques and Heat-Transfer Results for Cast-Cored Air-Cooled Turbine Blades. NACA RM E56C06, 1956.

2. Glenny, E.: The Application of the Investment-Casting Technique to the Manufacture of Blade Shapes Containing Cooling Fluid Passages. Memo. No. M.122, British NGTE, Dec. 1951.

3. Ainley, D. G., Waldren, N. E., and Hughes, K.: Investigations on an Experimental Air-Cooled Turbine. II - Cooling Characteristics of Blades Having a Multiplicity of Small Diameter Coolant Passages. Rep. No. R.154, British NGTE, Mar. 1954.

4. Ainley, D. G.: The High Temperature Turbo-Jet Engine. Jour. Roy. Aero. Soc., vol. 60, no. 549, Sept. 1956, pp. 563-581; discussion, pp. 581-589.

5. Ellerbrock, Herman H., Jr., and Stepka, Francis S.: Experimental Investigation of Air-Cooled Turbine Blades in Turbojet Engine. I - Rotor Blades with 10 Tubes in Cooling-Air Passages. NACA RM E50I04, 1950.

6. Curren, Arthur N., and Cochran, Reeves P.: A Balanced-Pressure Sliding Seal for Transfer of Pressurized Air Between Stationary and Rotating Parts. NACA RM E56I11, 1957.

7. Stepka, Francis S., and Hickel, Robert O.: Methods for Measuring Temperatures of Thin-Walled Gas-Turbine Blades. NACA RM E56G17, 1956.

8. Schafer, Louis J., Jr., and Hickel, Robert O.: Analytical Determination of Effect of Turbine Cooling-Air-Impeller Performance on Engine Performance and Comparison of Experimentally Determined Performance of Impellers with and without Inducer Vanes. NACA RM E54H12, 1954.

9. Ellerbrock, Herman H., Jr., Schum, Eugene F., and Nachtigall, Alfred J.: Use of Electric Analogs for Calculation of Temperature Distribution of Cooled Turbine Blades. NACA TN 3060, 1953.

10. Brown, W. Byron, and Donoughe, Patrick L.: Extension of Boundary-Layer Heat-Transfer Theory of Cooled Turbine Blades. NACA RM E50F02, 1950.

11. Hubbartt, James E., and Schum, Eugene F.: Average Outside-Surface Heat-Transfer Coefficients and Velocity Distributions for Heated and Cooled Impulse Turbine Blades in Static Cascades. NACA RM E50L20, 1951.

4466

12. Boelter, L. M. K., Martinelli, R. C., Rowie, F. E., and Morrin, E. H.: An Investigation of Aircraft Heaters. XVIII - A Design Manual for Exhaust Gas and Air Heat Exchangers. NACA WR W-95, 1945. (Supersedes NACA ARR 5A06.)

13. Slone, Henry O., Hubbartt, James E., and Arne, Vernon L.: Method of Designing Corrugated Surfaces Having Maximum Cooling Effectiveness Within Pressure-Drop Limitations for Application to Cooled Turbine Blades. NACA RM E54H20, 1954.

14. Linke, W., und Kunze, H.: Druckverlust und Wärmeübergang im Anlauf der turbulenten Rohrströmung. Allgemeine Wärmetechnik, Jahrg 4, Heft 4, 1953, pp. 73-79.

15. Hubbartt, James E., Slone, Henry O., and Arne, Vernon L.: Method for Rapid Determination of Pressure Change for One-Dimensional Flow with Heat Transfer, Friction, Rotation, and Area Change. NACA TN 3150, 1954.

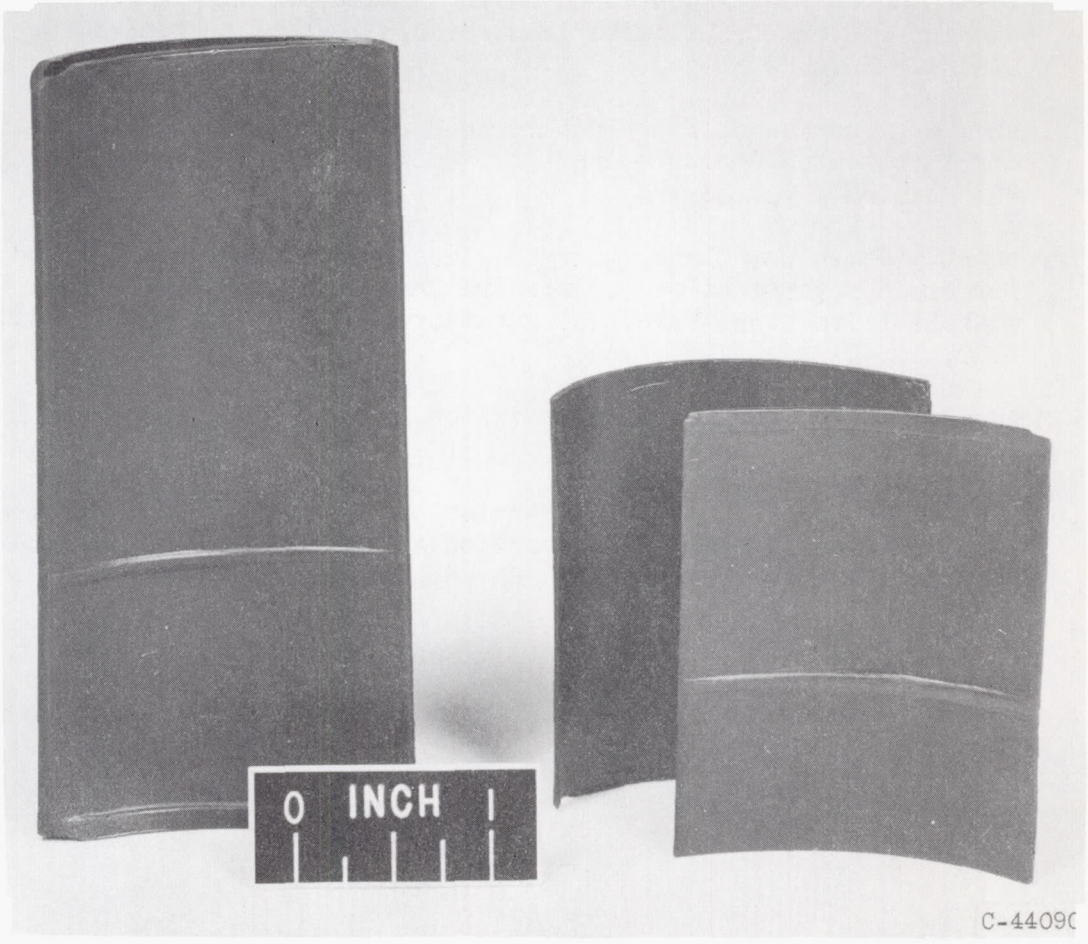
16. McAdams, William H.: Heat Transmission. Second ed., McGraw-Hill Book Co., Inc., 1942.

17. Schum, Eugene F., and Stepka, Francis S.: Analytical and Experimental Investigation of a Forced-Convection Air-Cooled Internal Strut-Supported Turbine Blade. NACA RM E53L22a, 1954.

4466

CA-3 back

4466

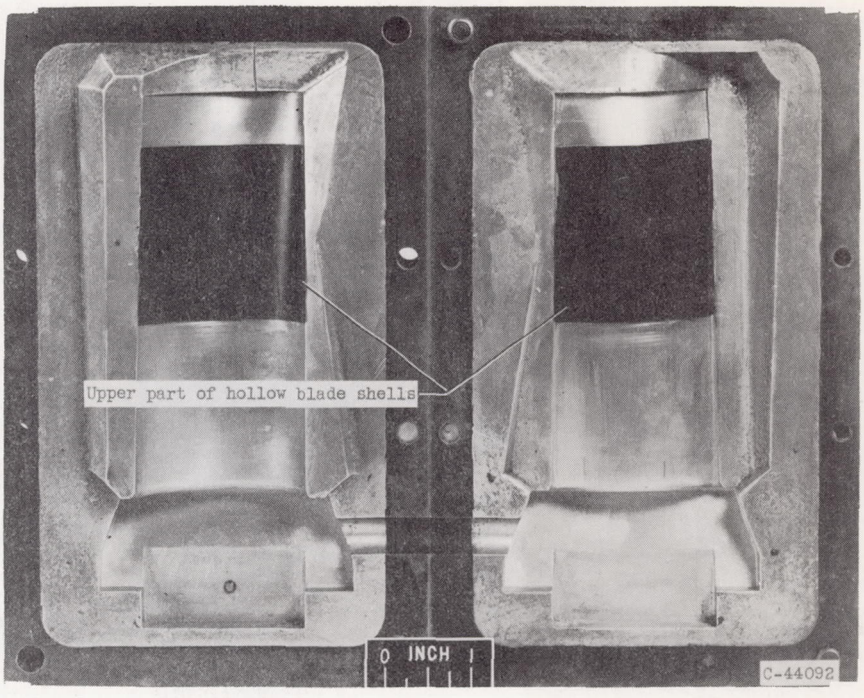


(a) Wax duplicate of hollow air-cooled blade.

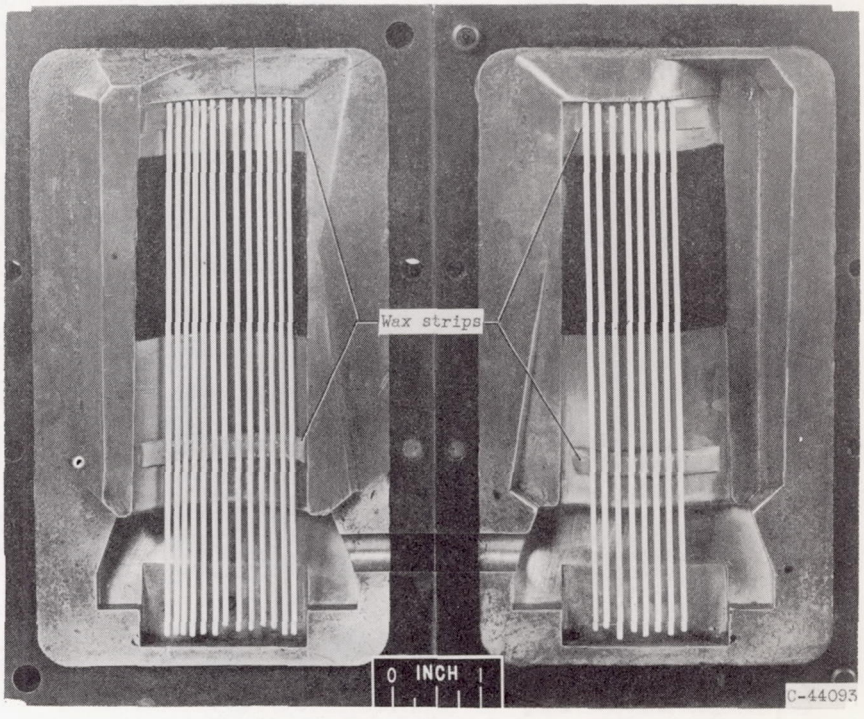
(b) Upper portion of hollow wax pattern split along leading and trailing edges.

Figure 1. - Alteration of wax duplicate of full-length hollow blade.

4466

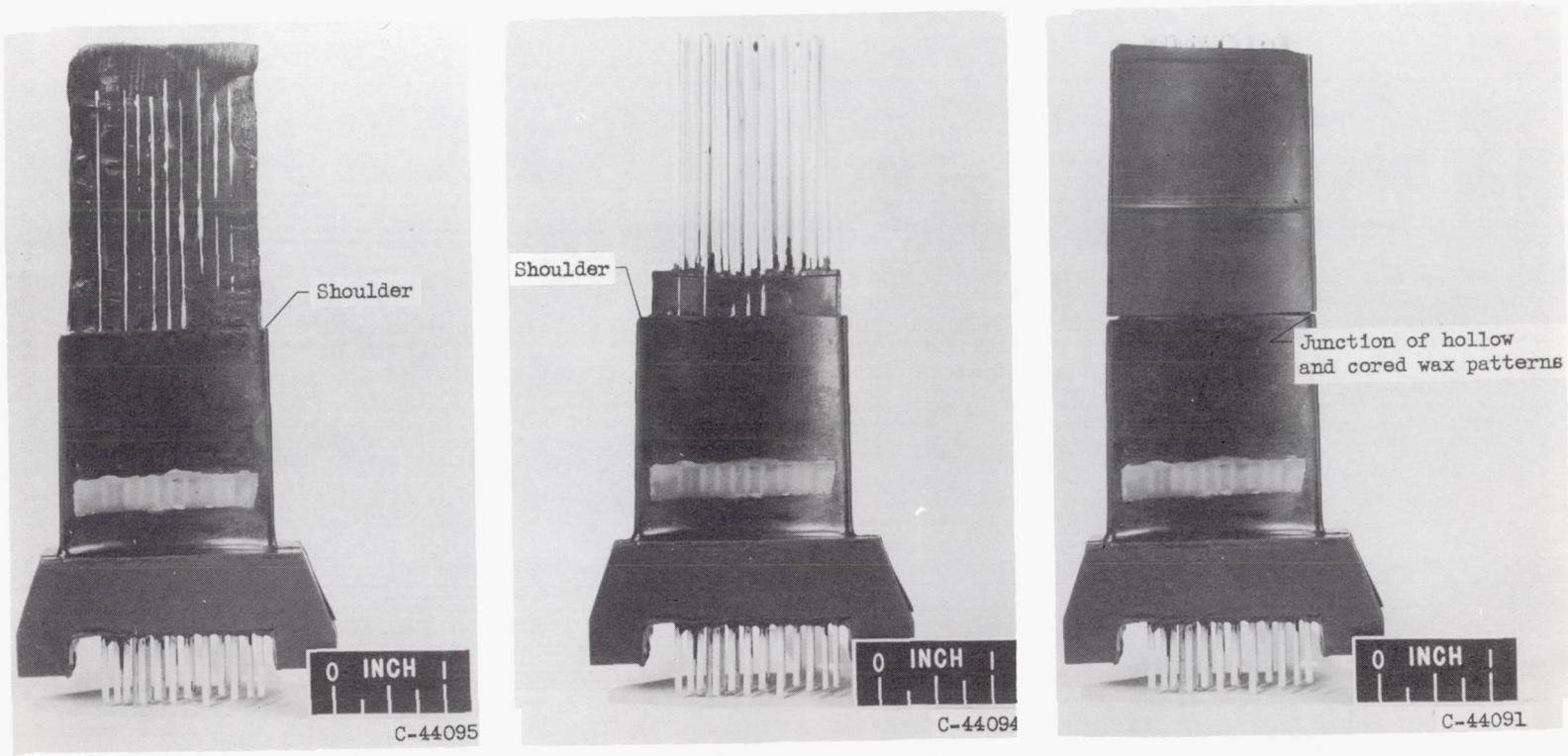


(a) Wax duplicates of upper part of hollow blade shells placed in die halves.



(b) Addition of two wax strips and ceramic cores to each die half.

Figure 2. - Assembly of hollow-blade-shell halves and ceramic cores in die halves.



(a) Wax pattern after removal from die. (b) Excess wax removed. (c) Final assembled wax pattern.

Figure 3. - Modifications of wax pattern and addition of hollow tip section required to produce wax duplicate of modified cast-cored blade.

4466

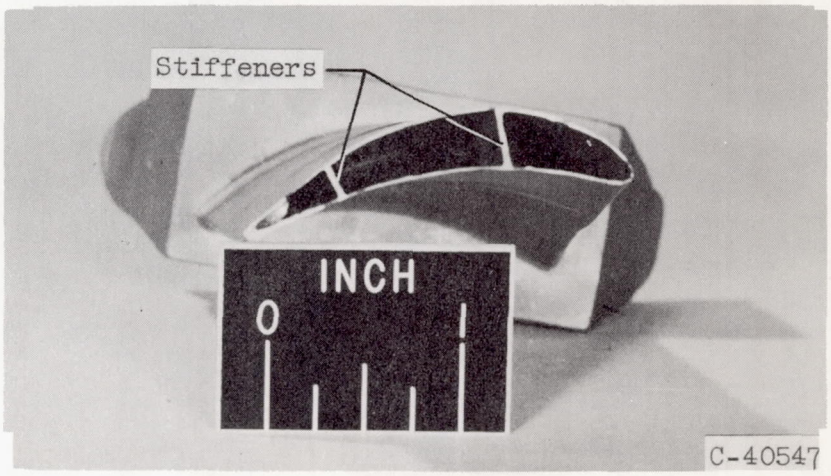
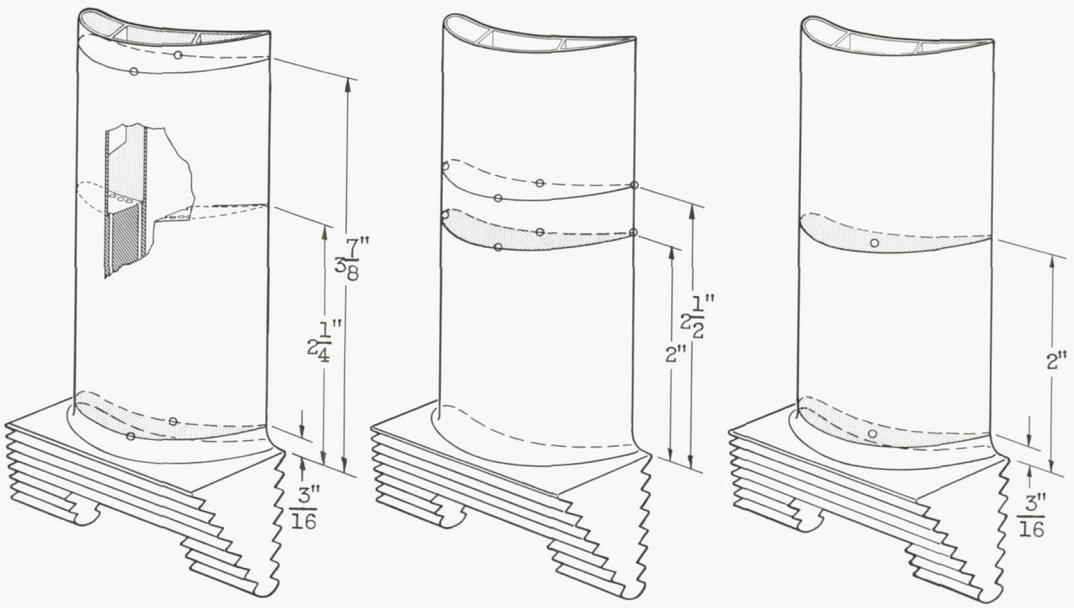
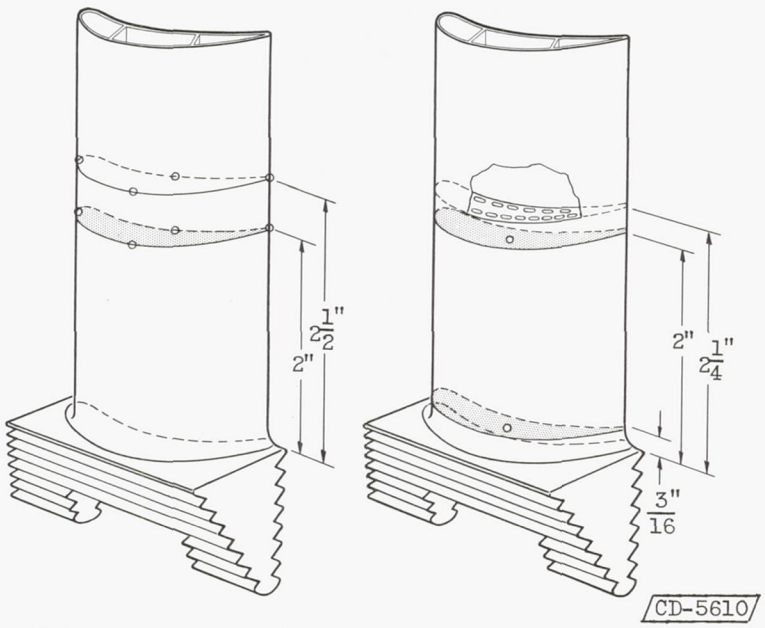


Figure 4. - Tip view of modified cast-cored blade showing stiffeners in hollow tip region.

4466

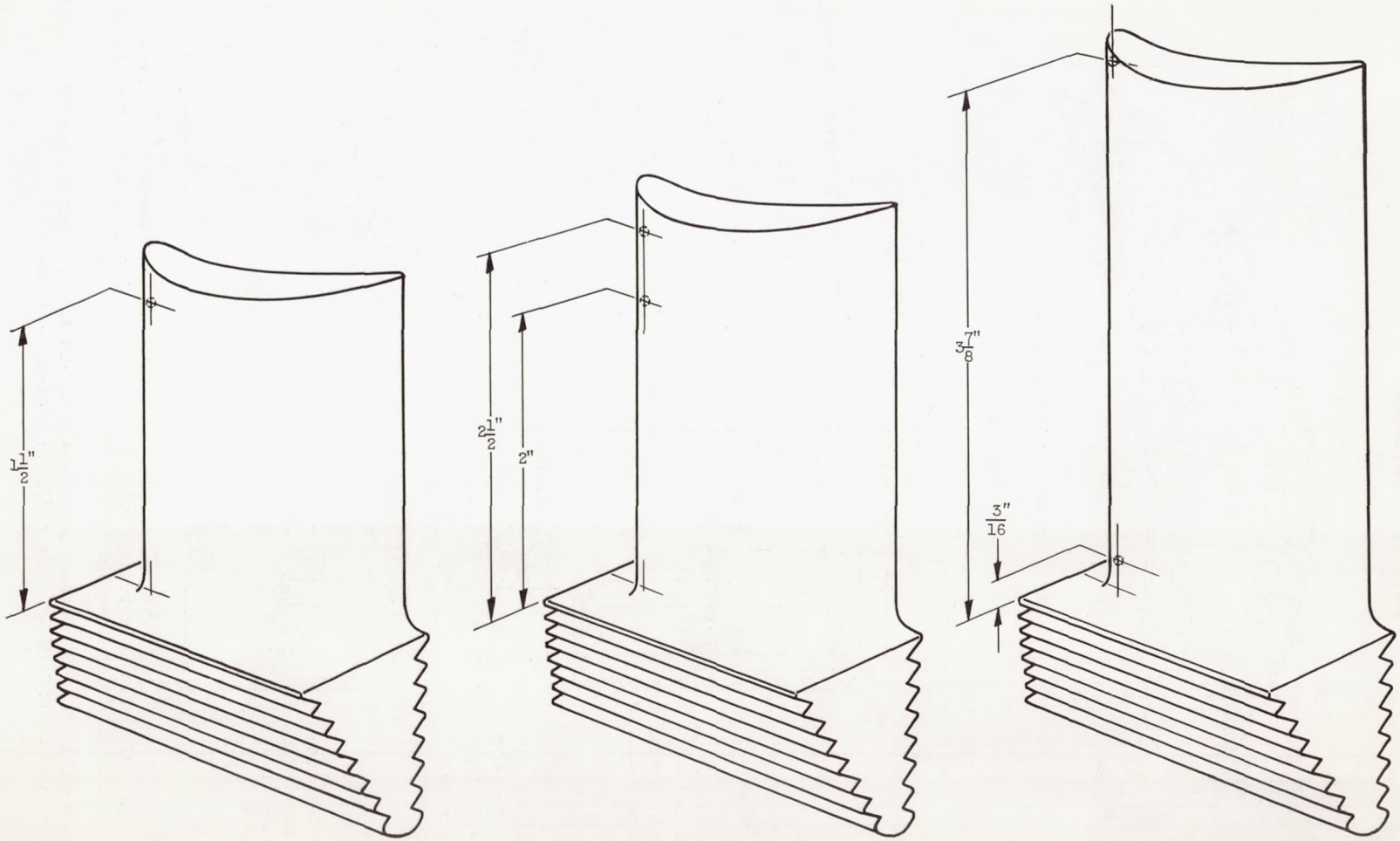


(a) Blade with 37 (0.060-in.) holes.



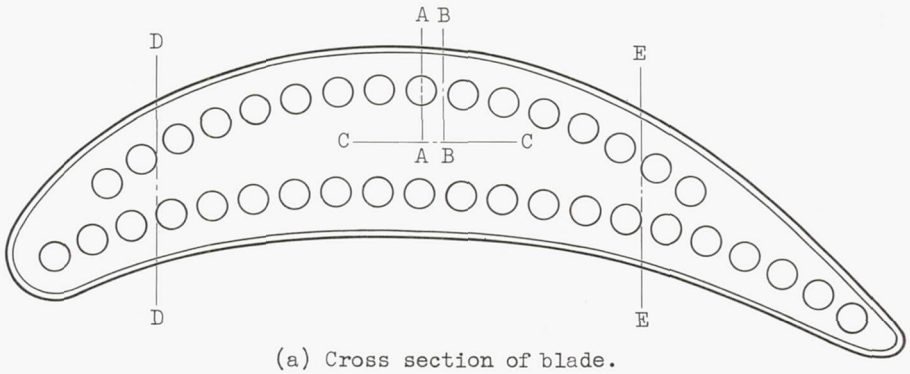
(b) Blade with 20 (0.060- by 0.100-in.) oval holes.

Figure 5. - Thermocouple installation on cooled and uncooled modified cast-cored blades.

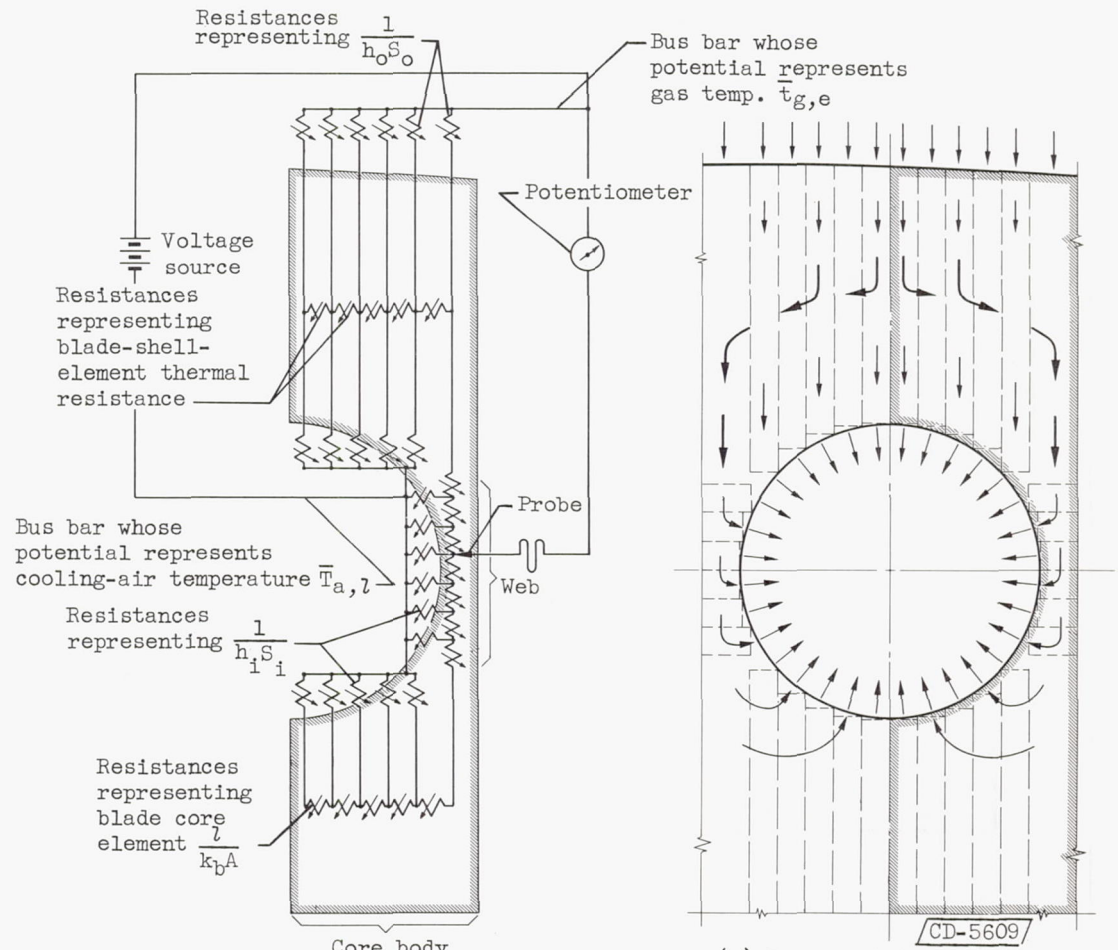


(c) Uncooled standard reference blades.

Figure 5. - Concluded. Thermocouple installation on cooled and uncooled modified cast-cored blades.



(a) Cross section of blade.



(b) Schematic illustration of analog wiring diagram.

(c) Representative section showing assumed heat-flow path.

Figure 6. - Sketches showing assumed heat-flow path and electric analog wiring diagram as applied to cross section of 37-hole modified cast-cored blade.

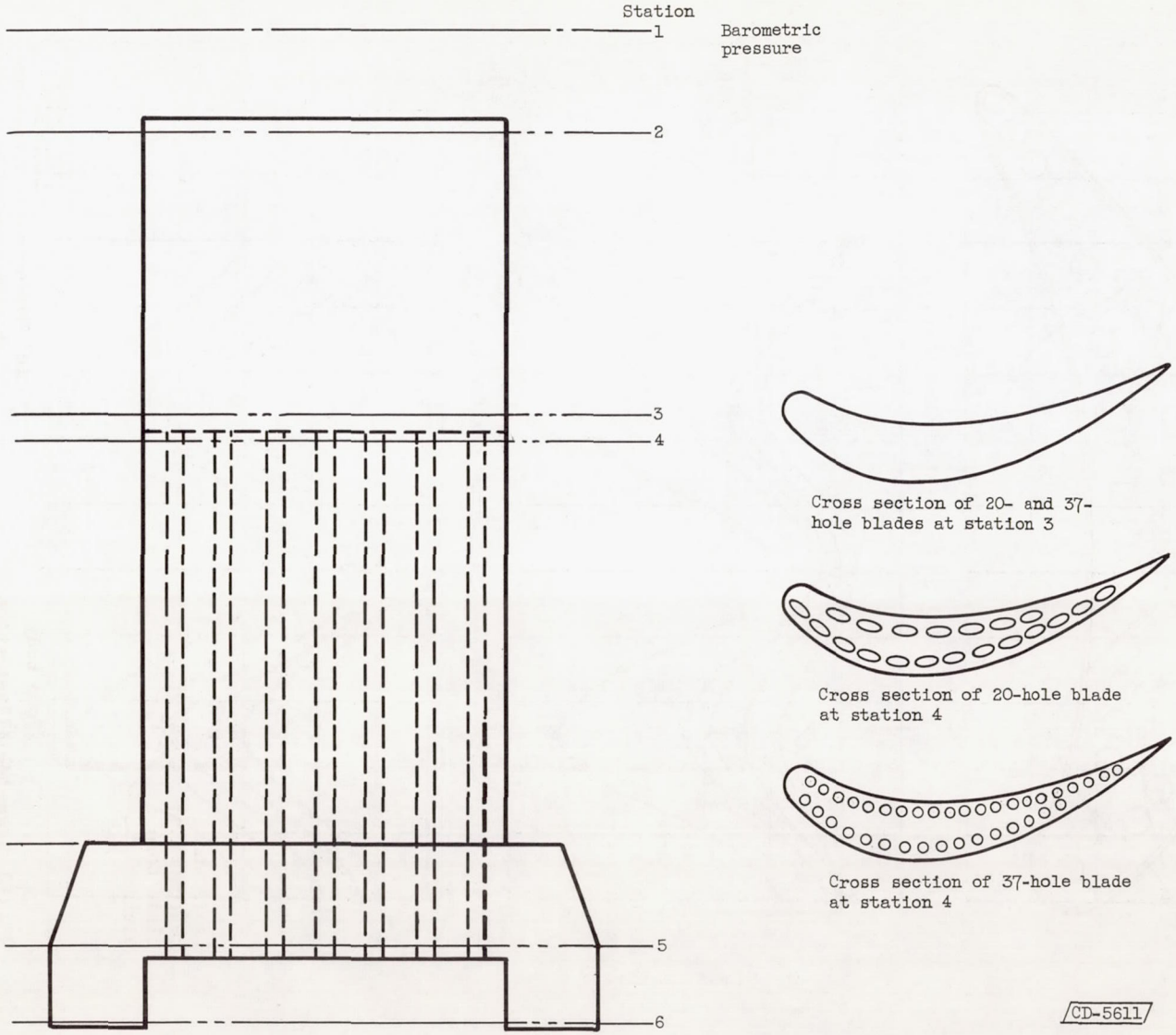
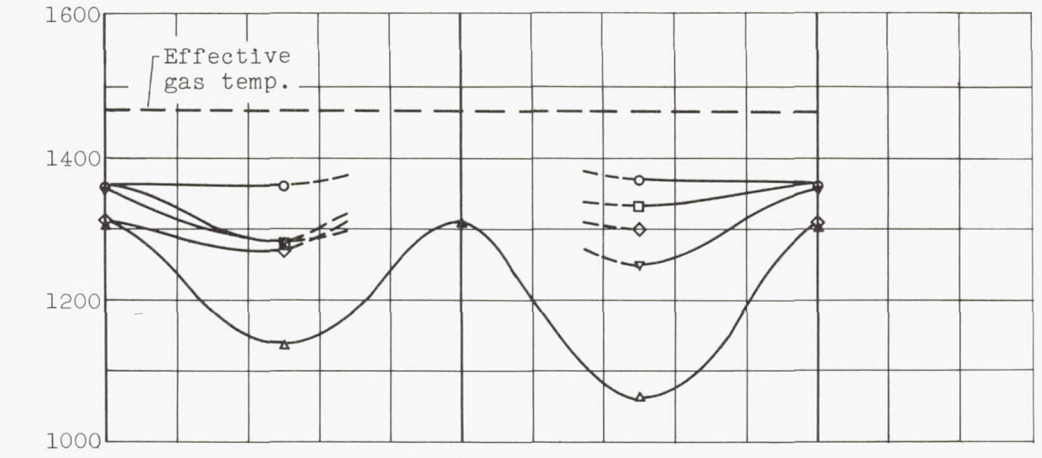
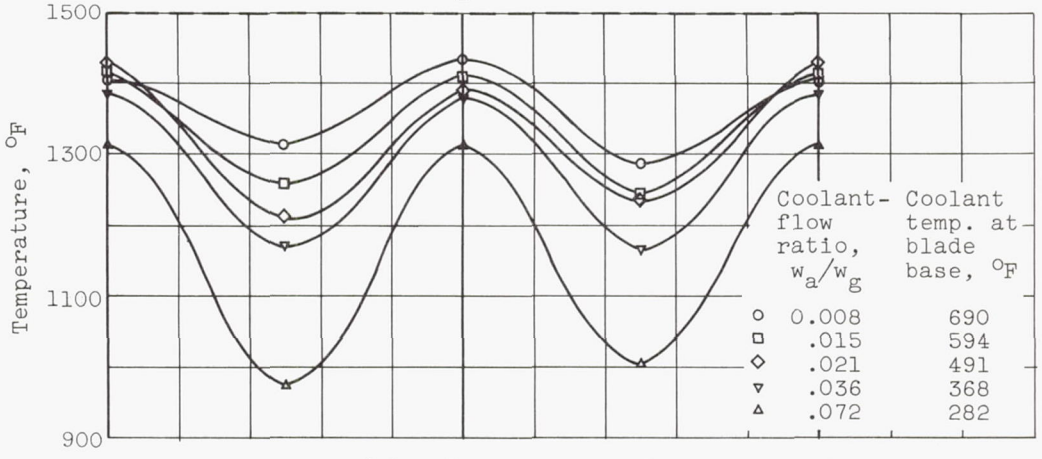


Figure 7. - Stations used in blade cooling-air pressure-drop calculations.

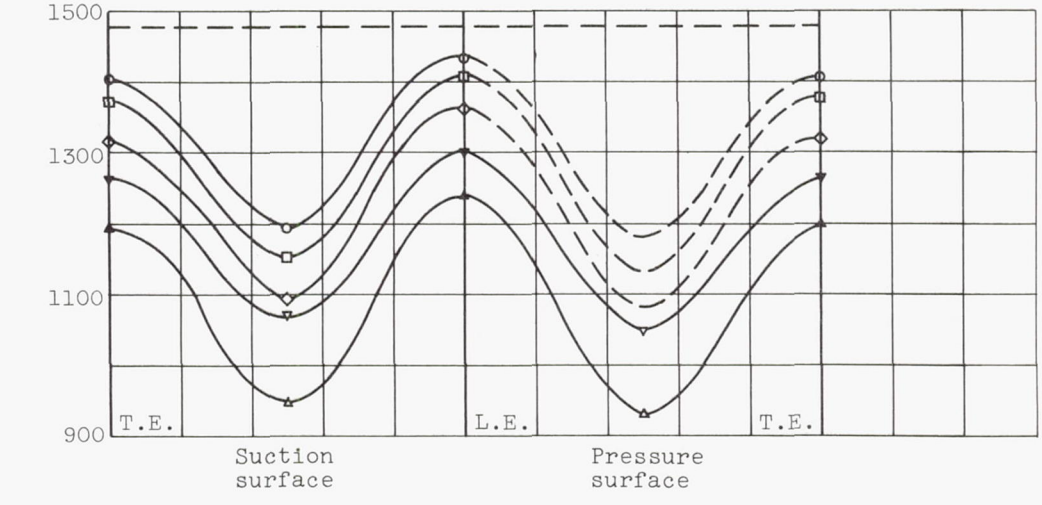
4466



(a) $2\frac{1}{2}$-Inch-span position.



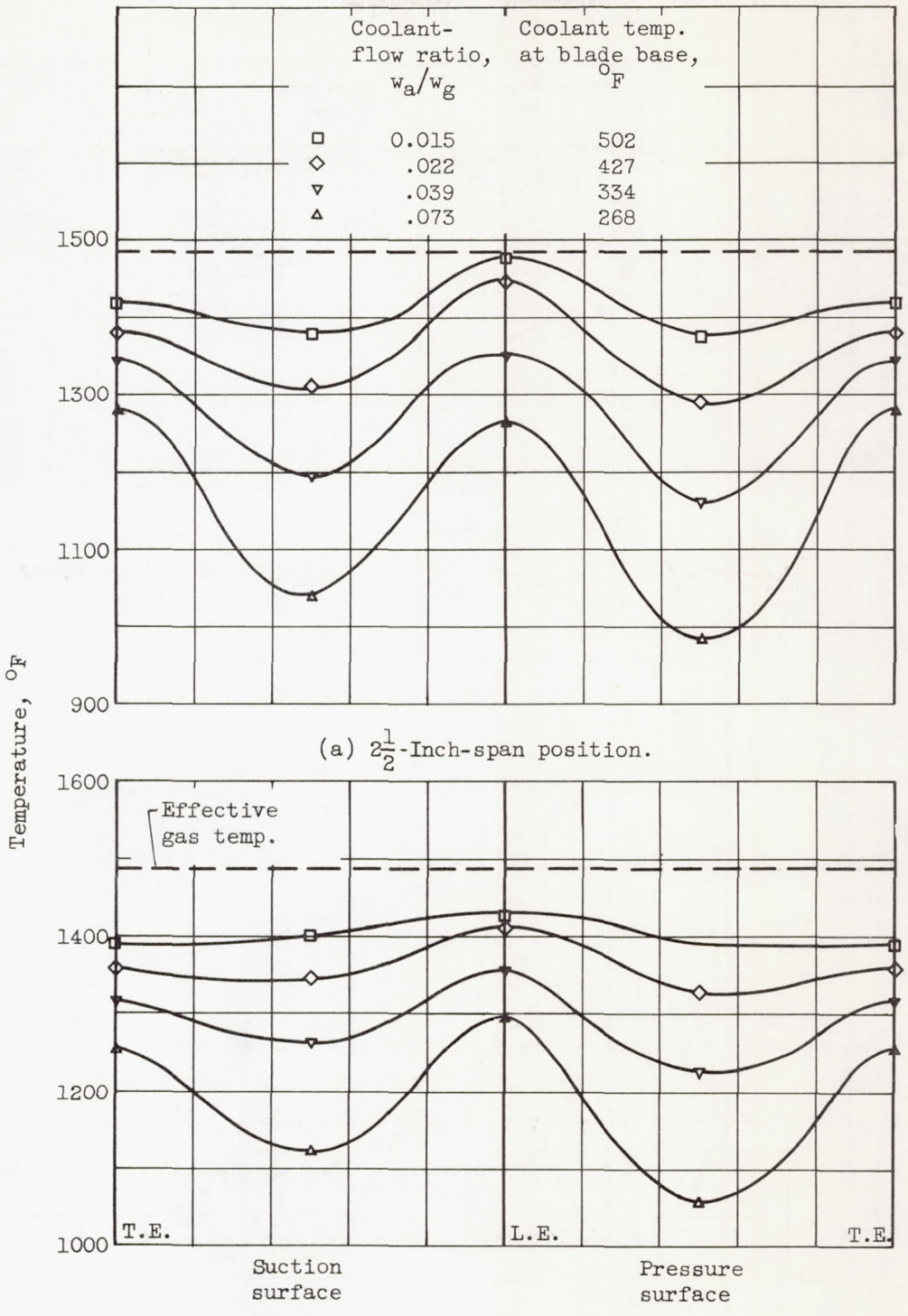
(b) 2-Inch-span position.



(c) 3/16-Inch-span position (root).

Figure 8. - Chordwise surface temperature distribution for hollow-tip blade with 37 (0.060-in.) holes. Engine speed, rated; turbine-inlet gas temperature, 1740° F.

4466

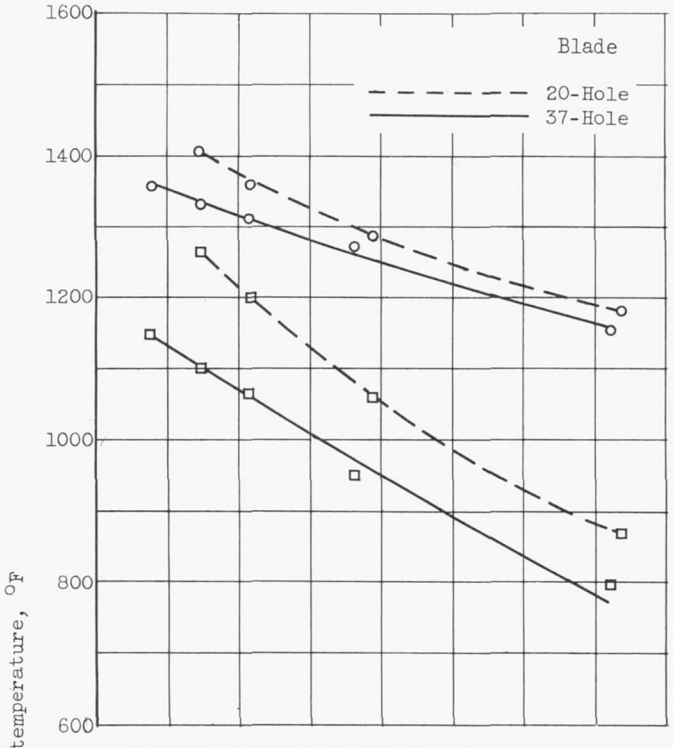


(a) $2\frac{1}{2}$-Inch-span position.

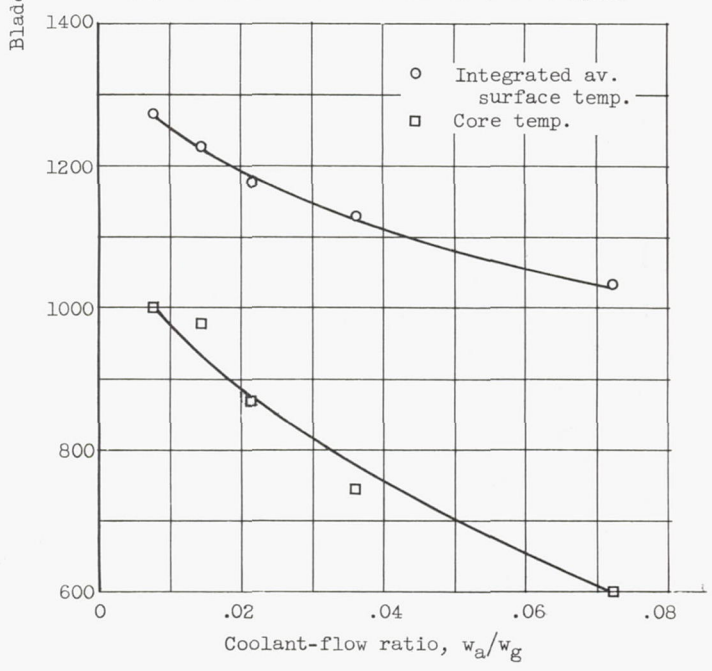
(b) 2-Inch-span position.

Figure 9. - Chordwise surface temperature distribution for hollow-tip blade with 20 (0.060- by 0.100-in.) holes. Engine speed, rated; turbine-inlet gas temperature, 1740° F.

4466



(a) 37- And 20-hole blades at 2-inch span.



(b) 37-Hole blade at root.

Figure 10. - Variation of integrated average surface temperature and metal core temperature with coolant-flow ratio for 37- and 20-hole modified cast-cored blades. Engine speed, rated; turbine-inlet gas temperature, 1740° F.

4466

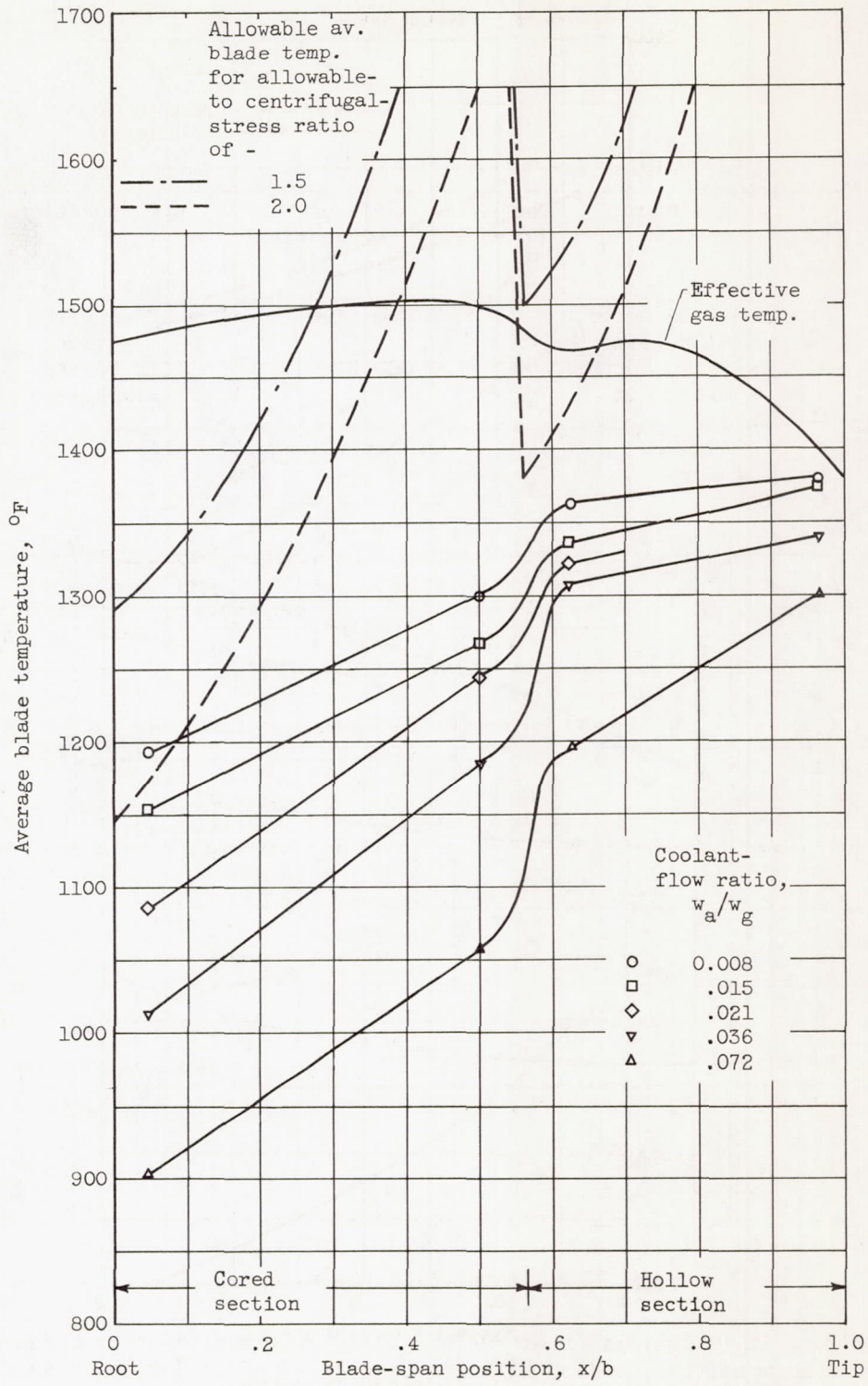


Figure 11. - Spanwise temperature distribution for hollow-tip blade with 37 (0.060-in.) holes. (Allowable blade temperature curves for 100-hour life superimposed when allowable-to centrifugal-stress ratios of 1.5 and 2 are specified.)

4466

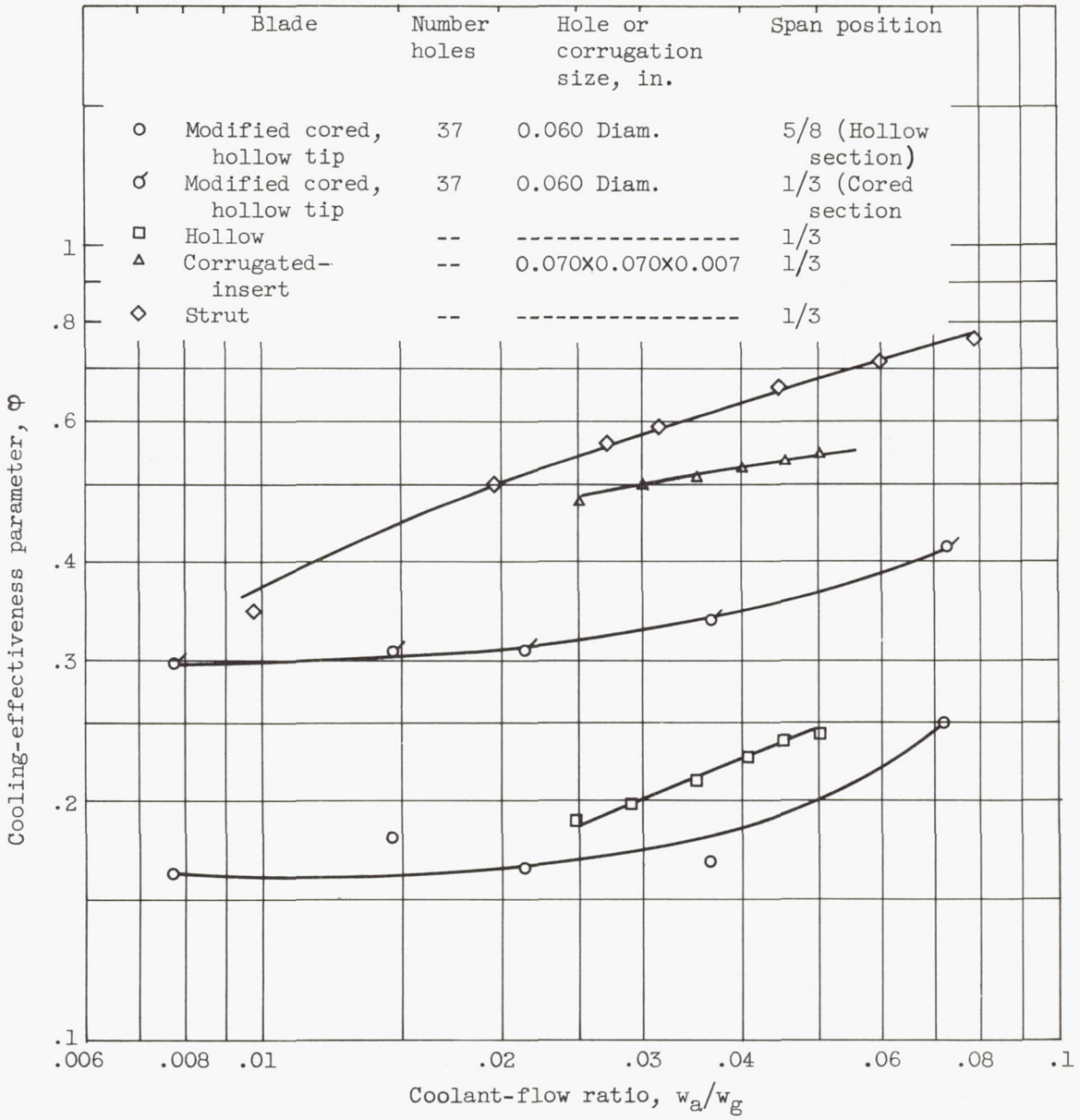
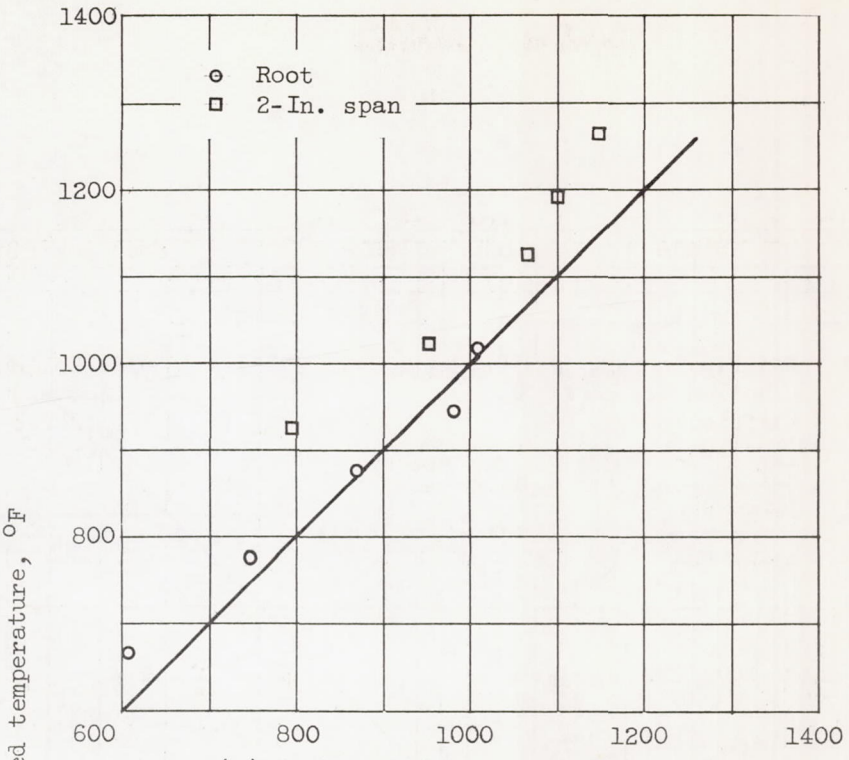
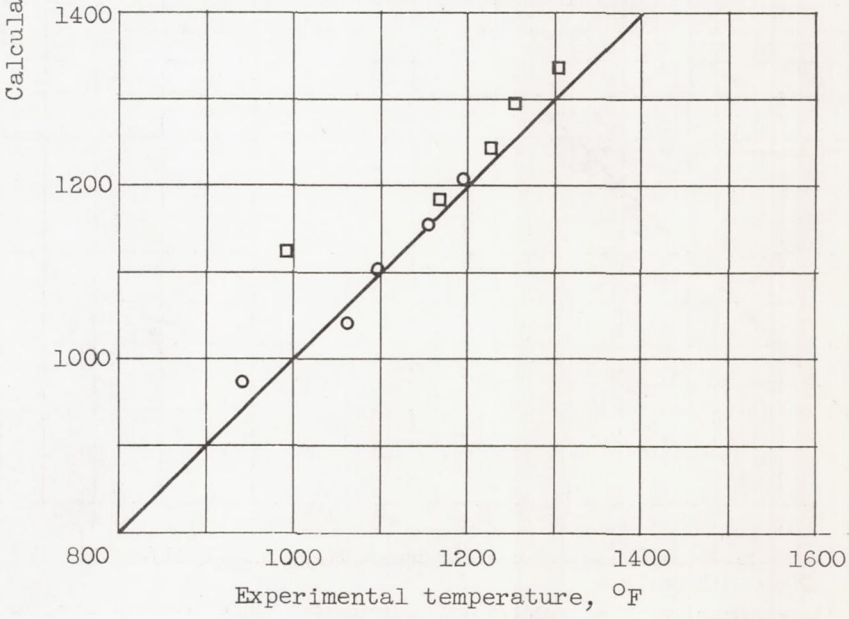


Figure 12. - Comparison of various blade configurations on basis of nondimensional cooling-effectiveness parameter. Engine speed, rated; turbine-inlet gas-temperature range, 1655° to 1740° F.



(a) Blade metal core temperatures.



(b) Surface midchord temperatures.

Figure 13. - Comparison of calculated and experimental blade temperatures for hollow-tip blade with 37 (0.060-in.) holes. Engine speed, rated; turbine-inlet gas temperature, 1740° F; coolant-flow-ratio range, 0.008 to 0.072.

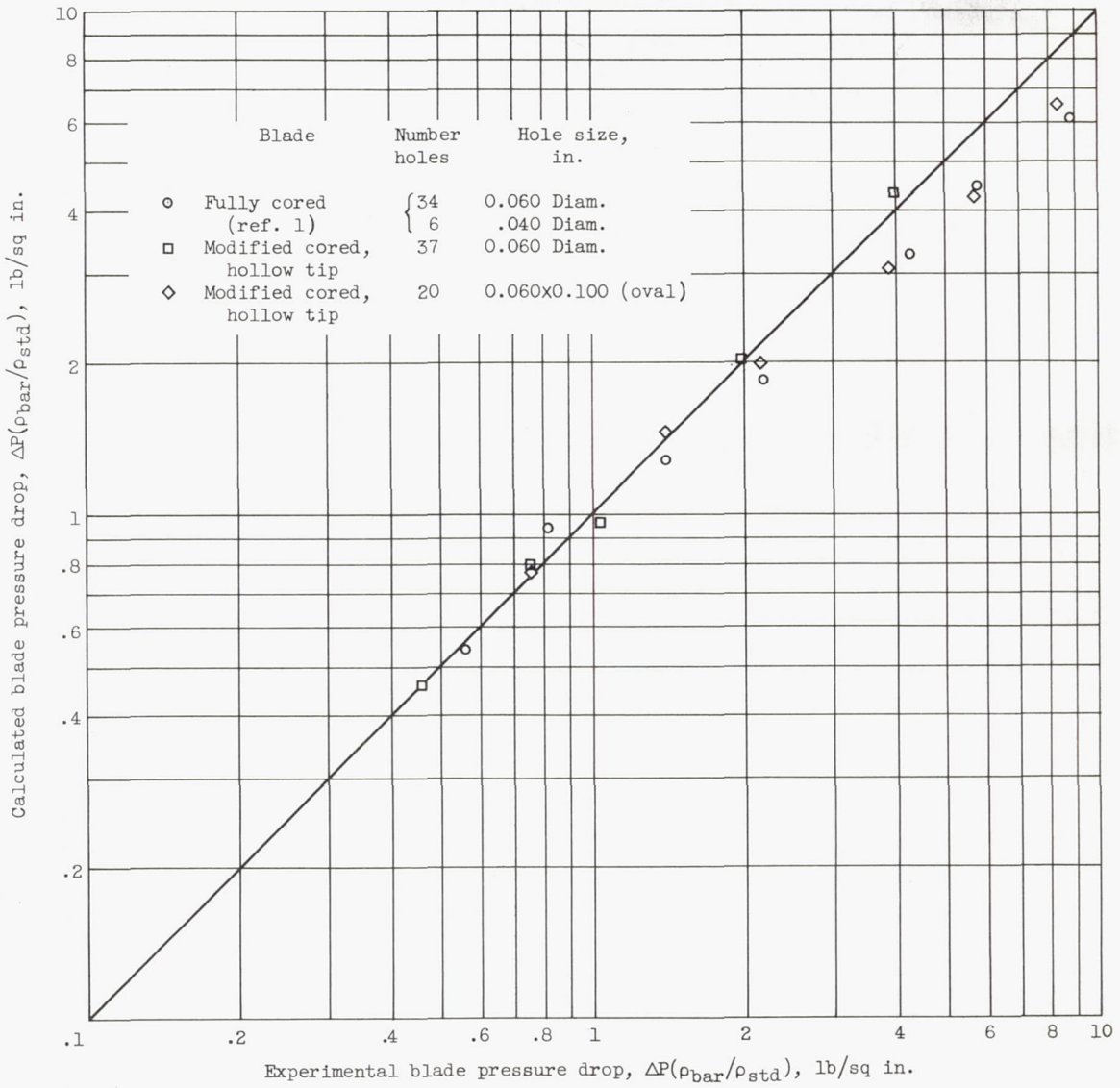


Figure 14. - Comparison of calculated and experimental blade pressure drop for fully cored and modified cast-cored blades.

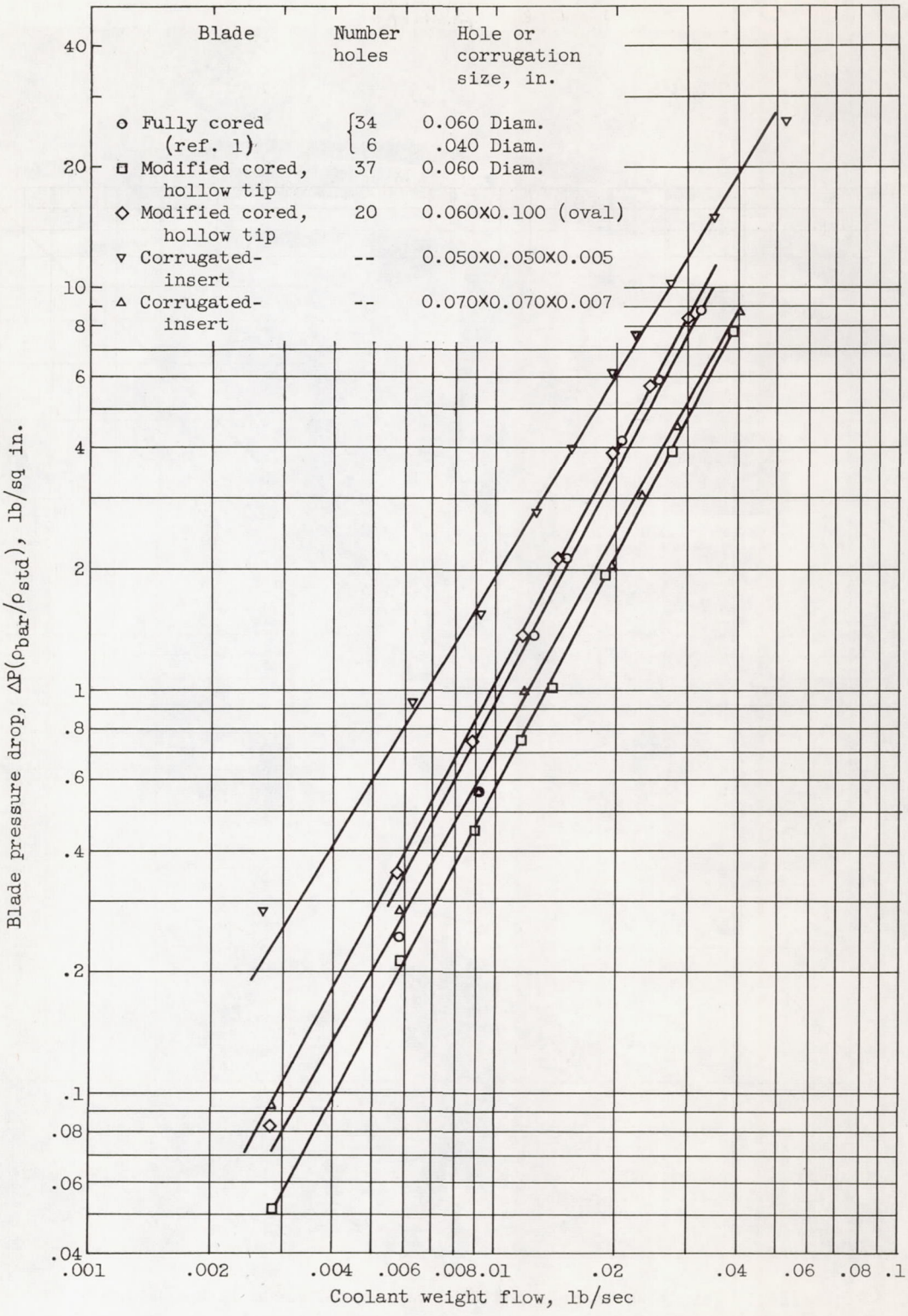


Figure 15. - Change in blade total-pressure drop with coolant weight flow for several air-cooled blade configurations.

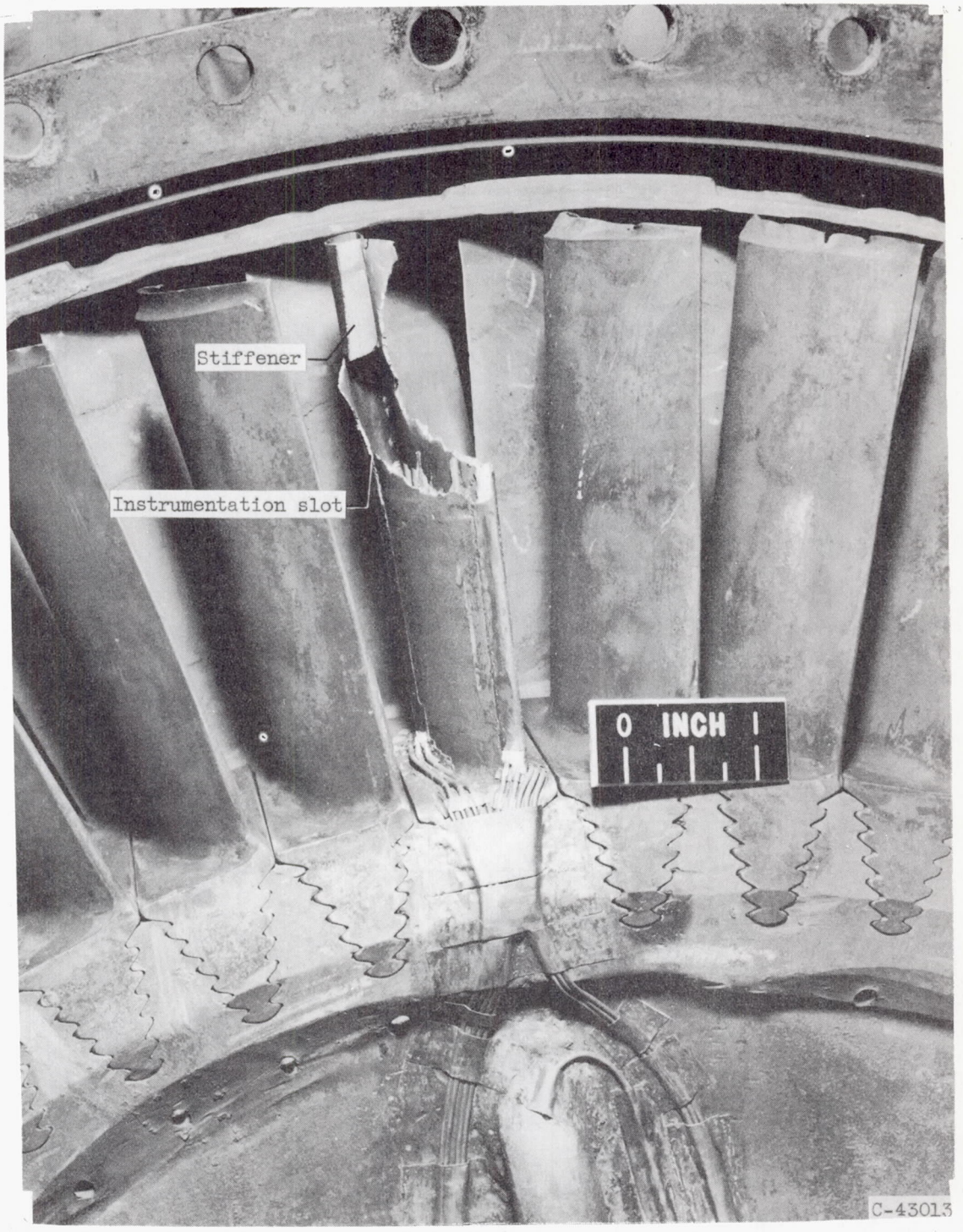


Figure 16. - Thirty-seven-hole modified cast-cored blade in engine after failure along instrumentation slot.